Clin Exp Metastasis (2009) 26:981–992
DOI 10.1007/s10585-009-9288-1

RESEARCH PAPER

Anti-metastatic effects of liposomal gemcitabine in a human orthotopic LNCaP prostate cancer xenograft model

Peter Jantscheff · Vittorio Ziroli · Norbert Esser · Ralph Graeser · Jessica Kluth · Alena Sukolinskaya · Lenka A. Taylor · Clemens Unger · Ulrich Massing

Received: 23 April 2009 / Accepted: 14 September 2009 / Published online: 26 September 2009

Abstract Fatal outcomes of prostate carcinoma (PCa) mostly result from metastatic spread rather than from primary tumor burden. Here, we monitored growth and metastatic spread of an orthotopic luciferase/GFP-expressing LNCaP PCa xenograft model in SCID mice by in vivo imaging and in vitro luciferase assay of tissues homogenates. Although the metastatic spread generally shows a significant correlation to primary tumor volumes, the susceptibility of various tissues to metastatic invasion was different in the number of affected animals as well as in absolute metastatic burden in the individual tissues. Using this xenograft model we showed that treatment with liposomal gemcitabine (GemLip) inhibited growth of the primary tumors (83.9 ± 6.4%; $P = 0.009$) as well as metastatic burden in lymph nodes (95.6 ± 24.0%; $P = 0.047$), lung (86.5 ± 10.5%; $P = 0.015$), kidney (88.4 ± 9.2%; $P = 0.045$) and stomach (79.5 ± 6.6%; $P = 0.036$) already at very low efficient concentrations (8 mg/kg) as compared to conventional gemcitabine (360 mg/kg). Our data show that this orthotopic LNCaP xenograft PCa model seems to reflect the clinical situation characterized by the fact that at time of diagnosis, prostate neoplasms are biologically heterogeneous and thus, it is a useful model to investigate new anti-metastatic therapies.

Keywords Adjuvant therapy · CEACAM6 · Liposomal gemcitabine · LNCaP · Metastases · Prostate cancer · SCID · Xenograft

Abbreviations

PCa	Prostate carcinoma
GemLip	Liposomal gemcitabine
Gemc	Gemcitabine
SCID	Severe combined immunodeficiency disease
dFdC	2′,2′-Difluoro-2′-deoxycytidine
RLU	Relative light units
ph/s	Photons per second
MTD	Maximal tolerable dose
EPR	Enhanced permeability and retention effect
GFP	Green fluorescent protein

Introduction

Prostate carcinoma (PCa) is the most frequent malignant tumor in males of western countries [1, 2] with

Electronic supplementary material The online version of this article (doi:10.1007/s10585-009-9288-1) contains supplementary material, which is available to authorized users.

P. Jantscheff · V. Ziroli · J. Kluth · A. Sukolinskaya · L. A. Taylor · U. Massing
Department of Clinical Research, Tumor Biology Center, Freiburg, Germany

N. Esser · R. Graeser
ProQinase GmbH, Freiburg, Germany

C. Unger
Clinic of Medical Oncology & Department of Clinical Research, Tumor Biology Center, Freiburg, Germany

P. Jantscheff (✉)
Clinical Research, Department of Lipids & Liposomes, Tumor Biology Center, Breisacher Str.117, 79106 Freiburg, Germany
e-mail: jantscheff@tumorbio.uni-freiburg.de

Present Address:
A. Sukolinskaya
N.N. Alexandrov National Cancer Center of Belarus, Minsk, Belarus

approximately 49,000 new cases (22.3% of male malignancies) and 11,000 deaths per year (i.e. 10.4% of all cancer deaths) alone in Germany [3]. Primary tumor burden, however, seems not to be the leading cause of cancer mortality since most deaths from PCa rather result from metastatic spread and its complications [4].

Advanced prostate cancer shows a strong metastatic capability with predilection to spread to the lymph nodes or bones but is also characterized by multiple organ metastases in lung, liver, kidney, and spleen [5–9]. Once prostate tumor cells are engrafted particularly in the skeleton, curative therapy becomes impossible and palliative treatment remains the only option [10]. For such advanced PCa, chemotherapy with the regimen mitoxantrone/prednisone as approved by the U. S. Food and Drug Administration (FDA) was commonly used, providing some symptom relief but no improvement in overall survival (OS).

Therefore, the development of new drugs, drug formulations or therapeutic strategies is a must for further progress in prostate cancer treatment [4]. Various experimental PCa models have been used for the investigation and development of new systemic adjuvant therapies against advanced PCa [11–18]. One way to establish such clinically relevant animal models accompanied by metastatic spread into bone or organ tissues was the orthotopic implantation of prostate cancer cells [13, 15, 19].

It has been demonstrated in such experimental models that various drugs (e.g. doxorubicin, taxanes) might display therapeutic efficacy by different mechanisms even when PCa cells are primarily insensitive to the drugs themselves. As shown in a recent study, an albumin-binding prodrug of doxorubicin that is cleaved by the serine protease activity of prostate-specific antigen (PSA) reduced tumor growth of orthotopical LNCaP xenografts [20]. This efficacy is probably due to the possibility of administering higher doses to tumor-bearing animals with simultaneously reduced side effects, accompanied by passive tumor targeting of albumin bound drugs mediated by the EPR, i.e. enhanced permeability and retention effect of macromolecules, since conventional doxorubicin failed in the model [20]. Taxanes also displayed beneficial efficacy in experimental PCa xenografts, probably resulting either from down-regulation of the expression of potent angiogenic factors (VEGF, bFGF) in the PCa tumor cells or direct effects on endothelial cells [21, 22].

Although displaying a resistant phenotype to e.g. doxorubicin in vitro, tumor cells from various tissues, e.g. from melanoma, non-small cell or small cell lung carcinoma have recently been shown to display enhanced sensitivity to gemcitabine (Gemc) (2′,2′-difluoro-2′-deoxycytidine, dFdC) [23]. Since cell lines or primary cells from advanced PCa are also often highly sensitive to low doses of Gemc in vitro (30–500 nM) [24–26], one might expect that Gemc to be a useful agent for the treatment of advanced, metastatic PCa in patients. Thus, it was quite astonishing that Gemc had only very limited effects on advanced PCa in clinical trials (maximum response rate: about 7%) [27–29].

Recently, we have shown that liposomal gemcitabine (GemLip) results in strongly increased cytostatic effectiveness and—in contrast to conventional gemcitabine—strongly inhibited tumor growth and metastatic lesions [30–32]. PK-studies with either liposomal or non-liposomal radioactively labelled gemcitabine clearly showed that the liposomal formulation as used in this study stably entrapped gemcitabine, extending its half-life from 9 min by more than 13 h. Tumor accumulation was improved by a factor of four in a sarcoma model growing in nude mice [30]. Furthermore, GemLip at much lower concentrations than free gemcitabine (Factor: 45) showed superior activity in two orthotopic pancreatic tumor models growing in nude mice, and was highly active towards metastases [31, 32].

Therefore, the goal of our study was to establish and characterize a highly metastatic PCa xenograft model using luciferase/GFP-transduced orthotopically implanted LNCaP cells and to investigate whether liposomal gemcitabine (GemLip) might be a new systemic option for anti-metastatic therapy in prostate cancer.

Methods

Cell culture and cell lines

PCa cell lines, LNCaP.FCG (ATCC, CRL-1740), Du145 (ATCC HTB-81), and PC-3 (ATCC CRL-1453) cells were routinely passaged in vitro in DMEM supplemented with 1% Glutamine, 1% Pen-Strep, 1% Fungizone (Invitrogen, Heidelberg, Germany) and 10% FCS (Cambrex, Verviers, Belgium) at 37°C with 10% CO_2 in a humidified atmosphere. The doubling times of PCa cells are very similar, i.e. cells display comparable proliferation properties, and account between 21.1 ± 4.7 h (PC-3), 25.7 ± 5.1 h (LNCaP) and 28.4 ± 12.2 h (Du145).

Determining the IC_{50} of GemLip and gemcitabine to LNCaP, Du 145, and PC-3

About 100 µl of the cells were seeded at 1×10^5/ml per well into 96 well plates (Greiner BioOne, Frickenhausen, Germany). After 24 h, another 100 µl of Gemc solution and GemLip dispersion were added at indicated final concentrations and the cells were incubated for another

48 h. Finally, BrdU reagent (Roche Diagnostics GmbH, Penzberg, Germany) was added for 4 h. Culture supernatants were removed, the cells were fix-dried for 1 h at 60°, and stored at 4°C. BrdU assays were performed according to manufacturer's instructions. Inhibition of DNA synthesis was calculated as percentage of BrdU incorporation compared to untreated cells. About 50% inhibitory concentration was calculated within the linear area of the inhibitory curve.

Generation of luciferase expressing PCa cells

To determine potential metastases and anti-metastatic effects of conventional Gemc or GemLip in vivo with high sensitivity in the mouse tissues [33] we established stably luciferase (Luc) or luciferase/GFP-transduced PCa cells.

The retrovirus encoding the Luciferase-aminoglycoside phosphotransferase (Neomycin resistance) or the Luc-GFP-Neo fusion protein was constructed from the luciferase gene of pUHC 13-3 (pTRE Luc, [34]), and the neomycin resistance gene from pcDNA 3.1 (Invitrogen, Heidelberg, Germany), using pLib (BD Clontech, Heidelberg, Germany) as a backbone. The EF1α was derived from a pEF vector (Invitrogen, Heidelberg, Germany), and introduced upstream of the Luci–Neo fusion gene. The GFP cDNA was isolated from pmaxGFP (Amaxa), and was inserted upstream of an IRES (internal ribosomal entry site) fragment wedged between the eGFP and the Luci–Neo fusion gene, allowing expression of both proteins from a bicistronic mRNA. The transduction of the LNCaP cells using a VSV-G (BD Clontech, Heidelberg, Germany) pseudotyped retrovirus was performed according to the instructions from the manufacturer. After selecting successfully transduced cells using 1 mg/ml Neomycin, their luciferase activity was tested. 10^6 cells were lysed in 100 µl in 1× luciferase lysis buffer (25 mM TRIS–phosphate pH 7.8; 2 mM for luciferase activity (Promega E4550), according to the manufacturer's instructions in a Luminometer (BMG Lumistar).

Preparation of gemcitabine liposomes (GemLip)

VPGs consisted of hydrogenated egg phosphatidylcholine/cholesterol (55:45 molar ratio; Lipoid AG, Ludwigshafen, Germany) at a total lipid concentration of 40% (m/m) (660 mM lipid). For each batch of VPG, 12 g lipid mixture was hydrated with 18 ml mannitol solution (5%), and treated with a high pressure homogenizer (Micron Lab 40, 70 Mpa, 10 cycles; APV Gaulin, Lübeck, Germany). The resulting "empty VPGs" were aliquoted into 30 ml injection vials (Zscheile & Klinger, Hamburg, Germany) in portions of 3.71 g. About 6 g glass beads (5 mm in diameter) were added as shaking aid, the vials were closed with a silicone rubber stopper, autoclaved at 121°C, 2 bar, 20 min and stored at 4–8°C [35].

For the entrapment of gemcitabine (Gemzar®; kindly provided by Lilly-Deutschland GmbH Bad Homburg, Germany) within the empty VPG, the "passive loading" technique was employed [36]. In short, 0.5 ml Gemc solution (38 mg/ml in 0.9% NaCl) was added to the VPG containing vials, the components were thoroughly mixed using a microdismembrator (1,500 shakes/min, 10 min), incubated for 1 h at room temperature and mixed a second time (1,500 shakes/min, 5 min). To ease the diffusion of Gemc into the liposomes, the mixtures were incubated at 60°C for 2 h in an aluminium block. Final Gemc conc. in the dual formulation is 19 mg/vial.

GemLip-VPG was diluted in 6.4 ml of a 0.9% sterile NaCl solution to yield a final total lipid concentration of 231 mM, and mixed (1,500 rpm, 10 min). The resulting GemLip was pushed through a 5 µm particle filter (Braun Melsungen AG, Melsungen, Germany) and further diluted for the animal injections.

Encapsulation efficiency of Gemc was analysed by the comparison of entrapped Gemc to total Gemc of each sample. Non entrapped Gemc was removed from GemLip by adsorption over a cationic exchange resin AG 50W X-8 (Bio-Rad, Munich, Germany) activated with concentrated NaCl. Eluted sample and non-eluted sample were dissolved in ethanol/methanol 90/10 (vol/vol) with a dilution factor of 200 to disintegrate the liposomes. Encapsulation efficiency (EE) was determined by Gemc-content ratio of these two samples. Gemc-content was standardized to the cholesterol content to correct for recovery after ion exchange chromatography. EE was calculated as the ratio of ([Gemc-]/[Chol]) Eluat sample/([Gemc-]/[Chol]) non-eluted sample * 100%.

Gemcitabine and cholesterol were simultaneously detected in one HPLC run by the use of a 2 column system: LiChrospher 60 RP-select B, endcapped, 5 µm, 250 × 4 mm (with a guard column 4 × 4 mm) and LiChrospher 100 NH2, 5 µm, 250 × 4 mm (both Merck, Germany). Mobile phase: Acetonitrile/Methanol/H2O acidified (containing 1% (w/v) formic acid, pH adjusted to 2.3) 67:30:3 (v/v/v). Flow 1.5 ml/min at 30°C. UV-detection: 0–6.5 min 278 nm (Gemc 4.9 ± 0.6 min), 6.5–10 min 215 nm (Chol 7.0 ± 0.1 min). Linear Calibration lines (peak area, fitted 1/x): Gemc 2–12 µg/ml ($r^2 = 0.9989 \pm 0.0011$), Chol 100–800 µg/ml ($r^2 = 0.9992 \pm 0.0009$). LOD 0.324 µg/ml (Gemc) and 6 µg/ml (Chol), respectively.

The manufacturing process was validated, taken in account the values of 16 batches (each comprising of 12 preparations in mean):

	Gemcitabine (mg/vial)	VPG (mg/vial)	Encapsulation efficiency (%)	Lyso-PC content (%)*	Liposome size (nm)**
Mean ($n = 192$):	19.4	3,652.9	46.3	4.2	36
SD	1.44	278.18	2.59	0.99	5

* Determind by HPTLC

** Determined by Photon correlation Spectroscopy, number weight Gaussian distribution

Animal experiments

All animal experiments were performed in accordance with German Animal License Regulations (Tierschutzgesetz) identical to UKCCCR Guidelines for the welfare of animals in experimental neoplasia [37]. 8–12 week old male SCID (C.B-17/IcrHanHad-Prkdc) mice were obtained from Charles River Laboratories, Sulzfeld, Germany.

Orthotopic LNCaP PCa xenografts were induced by injecting 1.00E+06 cells per animal in 25 µl DMEM (Invitrogen, Heidelberg, Germany) into the left or right anterior prostate gland of SCID mice (C.B-17/IcrHanHad-Prkdc). Successful implantation and orthotopic tumor growth was monitored by in vivo bioluminescence (see below). Subcutaneous PCa xenografts were induced by injecting 2.00E+06 cells per animal in 50 µl DMEM/Matrigel (BD, Heidelberg, Germany) subcutaneously into the left flank of SCID mice (C.B-17/IcrHanHad-Prkdc). Tumor sizes were measured three times weekly via calliper ing and compared to Luciferase imaging. Tumor volume was calculated by the formula A × B × A/2, A being the major and B the minor diameter. Take rate was >95% for $LNCaP_{subcutaneous}$.

For chemotherapeutic intervention in orthotopic xenografts animals were randomized on day 23 after implantation by luminescence intensity (see below) into the 3 treatment groups (10 mice per group) eliminating the largest and the smallest primary tumors. In pre-experiments the maximal tolerable dose (MTD) in tumor-free SCID mice has been determined to be 8 and 360 mg/kg for GemLip and Gemc, respectively (not shown). Treatment groups received 8 mg/kg GemLip and 360 mg/kg Gemc intravenously. Additionally, one group was treated with the drug vehicle (physiol. NaCl) only. Animals were treated three times once weekly. In the vehicle control group one animal died out of other than experimental reasons.

Analysis of the tumor vessel permeability (Evans blue in vivo vascular leakage assay)

In vivo tumor vessel permeability and vascular volume were quantified by measuring Evans blue extravasation [38, 39]. Mice were injected intravenously with 100 mg/kg of Evans blue (10 mg/ml in 0.9% NaCl). After 30 min, the mice were sacrificed, blood samples as well as samples from tumor and skeletal muscle were taken, weighed and homogenized in 1/9 parts (w/w) of an 0.1% sodium sulfate/acetone mixture (3:7 v/v). After 17 h incubation at room temperature in the dark, the samples were centrifuged at 1,000×*g* for 5 min. The absorbance at 620 nm was determined in each supernatant, and the concentration of Evans blue was quantified using a standard. The amount of Evans blue in the tumor tissue and skeletal muscle values were calculated per tissue weight, and standardized for the measured blood concentration, furthermore, the Evans blue tumor to skeletal muscle ratios were determined.

Measurement of in vivo bioluminescence

About 100 µl of the substrate, D-Luciferin (20 mg/ml; Synchem OHG, Germany), were injected i.p. in two portions of 50 µl each, and the animals were then anesthetized in an isofluorene chamber. About 10 min later they were transferred into the Nightowl LB981 camera system (Berthold, Bad-Wildbach, Germany), and exposed for 1 min at 2 × 2 binning, and 5 min at 10 × 10 binning. For quantification of light signals bioluminescence was analyzed on raw images from the camera using the internal software "WinLight32" (Berthold, Bad-Wildbach, Germany) and expressed as photons/second (ph/s).

Quantification of metastatic lesions by in vitro luciferase assay

To screen and quantify metastatic lesions in potential target organs of SCID mice pieces of lung, liver, spleen, lymph node, stomach, kidney, femur, lumbar spine or duodenum were homogenized in 1 ml (liver in 5 ml) of luciferase lysis buffer using a tissue homogenizer Fastprep-24 and Lysing MatrixA tubes (MP Biomedicals, Heidelberg, Germany). Insoluble material was spun down for 10 min at 15,000 rpm in a Heraeus Biofuge15. About 5 µl of the supernatant were checked for protein concentration using a Bradford assay (Sigma B6916) with BSA serving as standard protein, and 10 µl were measured in a luciferase assay (Promega E1501). Data are shown as log RLU (relative light units) normalized by protein concentration.

Statistics

Statistical analyses were performed using student's *t*-test and paired *t*-test, respectively, or—if Normality Test failed—using Mann–Whitney Rank Sum Test (SigmaStat 3.1). Pearson Correlation (SigmaStat 3.1) was used to define relationships between tumor volume and metastatic spread. Testing to define if a population follows a standard, "bell" shaped Gaussian distribution, also known as a "normal" distribution was performed with the Normality Test (Kolmogorov–Smirnov) (SigmaStat 3.1).

Results

Sensitivity of LNCaP cells to GemLip in vitro

First, we investigated the effects of liposomal (GemLip) and conventional gemcitabine on various PCa cells in vitro. Efficiency of the drugs was determined by adding different concentrations of the drug formulations to LNCaP PCa cells for 24–120 h and compared to Du145 and PC-3 PCa cells. Empty liposomes at equivalent dosages as GemLip did not change BrdU incorporation in comparison to vehicle control (not shown). Optimal logarithmic growth was seen at 48 h and proliferation inhibition was analyzed at this time point using BrdU assay. We confirmed (Fig. 1, right) that luciferase-transduced PCa cells (LNCaP, Du145, PC-3) are also highly sensitive (IC50 10–30 nM) to conventional Gemc [24, 25]. As shown further (Fig. 1, left) the liposomal formulation GemLip displayed similar IC50 values in vitro. There were neither strong differences between the various PCa cells nor between GemLip and Gemc, respectively (IC50 LNCaP G/GL 11.0 ± 0.5/16.0 ± 0.5 nM, Du145 11.9 ± 3.1/20.5 ± 3.3 nM, and PC-3 14.9 ± 1.1/21.5 ± 1.6 nM). Despite of transduction and selection with G418 (1 mg/ml), the stably luciferase-transduced PCa cells did not exhibit any different sensitivity to Gemc or GemLip compared to parental cells (not shown).

In vivo properties of PCa xenografts: tumor growth and vascular leakage

To characterize in vivo properties of the transduced LNCaP cells we compared growth, vascular leakage, and metastasizing properties of ectopic subcutaneous and orthotopic xenografts, respectively. Tumor growth was determined either by measurement of the in vivo bioluminescence in the case of the orthotopic implantation or by callipering in the subcutaneous models (supplemented by bioluminescence).

The first palpable subcutaneous LNCaP tumors in the ectopic model were detected between days 10 and 12. Nearly all (>95%) animals developed subcutaneous tumors. Requirements for the possible commencement of therapeutic intervention, i.e. a tumor volume of >0.1 cm^3, were achieved between days 19 and 21. Tumor volumes larger than 1 cm^3, which are the ethical stop criterion, had developed in the animals between days 32 and 35, opening a potential therapeutic window of about 14 days only (Fig. 2a). Final tumor volume at necropsy was 1.53 ± 0.65 cm^3.

Bioluminescence of orthotopic xenografts was first determined between days 3 and 5 and next between days 10 and 13 after implantation into the anterior prostate gland. The take rates for $LNCaP_{ortho}$ xenografts were about 65%. Further tumor growth was monitored by bioluminescence once weekly (Fig. 2a). Stop criteria in the orthotopic models were the general health situation (scrubby coat) and body weight reduction (>20%) of the animals. As determined in this study, tumor growth was limited to days 54-

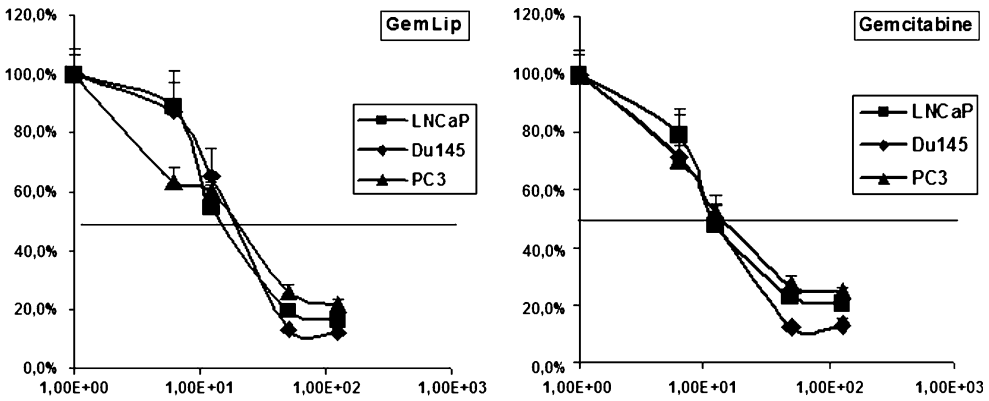

Fig. 1 IC50 values on LNCaP PCa cells of GemLip and gemcitabine in vitro. LNCaP and as control Du145 as well as PC-3 cells were incubated with GemLip, Gemc or the vehicle control (NaCl) for 24–120 h at designated concentrations. Optimal logarithmic growth was seen with all cells at about 48 h. Results from 3 independent experiments are shown as percentage of proliferation (BrdU) of the vehicle control at 48 h. The IC50 values cells were very similar for LNCaP 11.0 ± 0.5/16.0 ± 0.5 nM, Du145 11.9 ± 3.1/20.5 ± 3.3 nM, and PC-3 cells 14.9 ± 1.1/21.5 ± 1.6 nM, using GemLip and Gemc, respectively

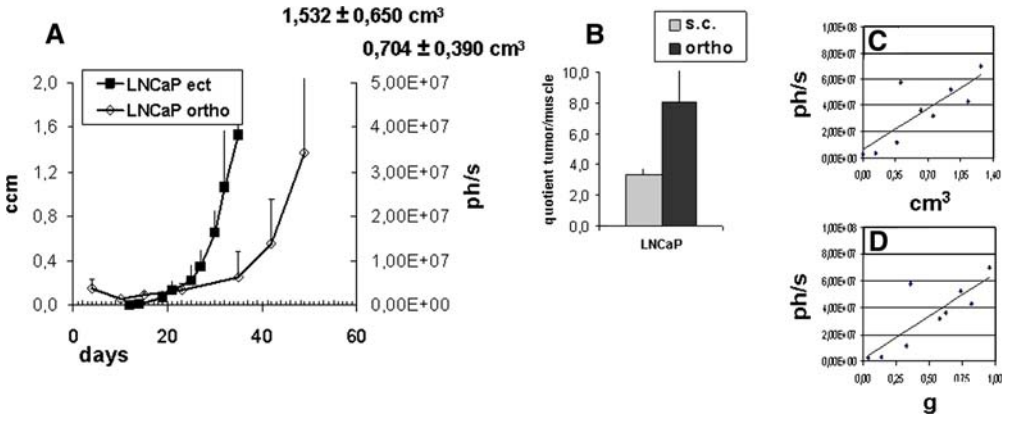

Fig. 2 Tumor growth curves and Evans Blue vascular leakage assay in orthotopic and subcutaneous LNCaP. Orthotopic LNCaP PCa xenografts were induced by injecting $2x10^6$ luciferase-transduced cells in 25 µl DMEM into the left or right anterior prostate gland of SCID mice (C.B-17/IcrHanHad-Prkdc), whereas ectopic LNCaP PCa xenografts were induced by injecting $2x10^6$ cells per animal in 50 µl DMEM/matrigel subcutanously into the left flank of SCID mice (C.B-17/IcrHanHad-Prkdc). Tumor growth was determined either by luciferase bioluminescence imaging, calculated as photons per second ± SD after exposure of 5 min at 10 × 10 binning or by callipering and calculated as mean ± SD by the formula D1 × D2 × D1/2 where D1 is the larger and D2 is the smaller diameter (A: LNCaP *filled black square* ectopic and *open diamond* orthotopic). At necropsy, final tumor volume was 1.532 ± 0.650 and 0.704 ± 0.390 cm^3 for ectopic and orthotopic tumors, respectively. Comparing imaging results and final tumor volume (**c**) or weight (**d**), a good correlation between bioluminescence (ph/s) and these two parameters could be shown [correlation coefficients are $R = 0.737$, $P = 0.037$ (cm^3) and $R = 0.821$, $P = 0.0066$ (**g**), respectively]. Tumor vessel permeability and vascular volume (**b**) was determined 30 min after Evans Blue i.v. application as tumor to skeletal muscle ratio in LNCaP orthotopic and subcutaneous PCa tumor xenografts in SCID mice. The tumor:muscle ratio was significantly augmented ($P < 0.05$) in orthotopic $LNCaP_{ortho} = 8.13 \pm 6.51$ ($n = 3$) (**b**: *black column*) compared to subcutaneous $LNCaP_{sc} = 3.31 \pm 0.48$ ($n = 3$) xenografts (**b**: *grey column*)

57 (Fig. 2a). This opened a general treatment window of about 31–34 days. The bioluminescent signal (ph/sec) at the end point analysis was about 20-fold higher than the randomization signal, corresponding to a final volume of orthotopic tumors of 0.70 ± 0.39 (LNCaP). Although showing a wide range, the luminescence values (34,330,542 ± 24,221,418) from final imaging of viable animals correlated well to tumor volume or weight at necropsy (Fig. 2c, d).

Tumor vessel permeability and vascular volume of PCa xenografts were quantified in vivo by measuring Evans blue extravasation [38, 39]. As shown in Fig. 2b (grey column) the Evans blue extravasation in the subcutaneous PCa xenografts in SCID-mice expressed as tumor to muscle ratio was about 3.31 ± 0.48 ($n = 3$). Comparing the vascular leakage of orthotopic PCa xenografts (Fig. 2b, black column) we could demonstrate that it was significantly ($P < 0.05$) augmented in the orthotopic situation [$LNCaP_{ortho} = 8.13 \pm 6.51$ ($n = 3$)].

Metastatic spread of ectopic and orthotopic LNCaP xenografts

No metastatic lesions were found in any of the tissues tested in mice with ectopic, i.e. subcutaneous, in 50% Matrigel implanted LNCaP xenografts grown for 32–35 days, even when using sensitive luciferase assays on the tissue homogenates (Fig. 3). The detection limit of the assay was between 100 and 1,000 transduced cells, i.e. 1,000–10,000 tumor cells per organ homogenized (Fig. 3).

In contrast to the above, when LNCaP cells were xenografted orthotopically, metastases were detected in untreated SCID mice. Macroscopic analyses during necropsy revealed metastatic lesions in spleen, lung and peritoneal cavity of some (1–2) animals (data not shown). However, sensitive in vitro luciferase assay of transduced cells detected metastatic lesions in homogenates of all investigated tissues of individual mice (Table 1). Metastatic burden was most prominent in lymph nodes, spleen, duodenum, or lung, and detectable at weaker amounts in femur and lumbar spine bone tissue samples, or kidney and liver, but varied not only in metastatic load in the individual tissue (i.e. mean RLU per tissue) but also in the number of metastatic animals (Table 1).

Although the range of metastatic burden in individual tissues was generally very high (Table 1), the distribution of metastatic lesions (Fig. 4, mean RLU) shows a significant correlation to the final primary tumor volume defined by imaging (Fig. 4, ph/sec) or by tumor volumes and weight, respectively (not shown), in individual animals. As shown in Fig. 3, the correlation was stronger in some [e.g. stomach ($R = 0.887$; $P < 0.0001$), lung ($R = 0.870$; $P < 0.0001$)] but also given in the other tissues [e.g. lumbar spine ($R = 0.510$; $P = 0.0181$) or femur ($R = 0.662$; $P = 0.0011$)].

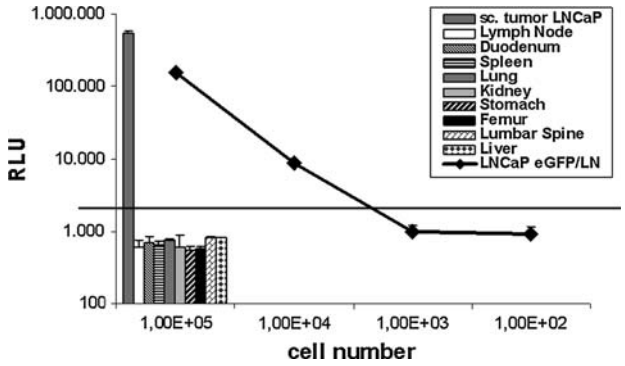

Fig. 3 Metastatic properties of ectopic subcutaneous LNCaP PCa xenografts. In vitro endpoint analysis using the highly sensitive luciferase assay—able to detect traces of at least 1.00E+02 to 1.00E+03 of luciferase-transduced LNCaP tumor cells in 100 µl equalling to a total amount of 1,000–10,000 cells per homogenized tissue piece in 1 ml (curves)—failed to reveal any significant signals in homogenates of lymph node, intestine tissue, spleen, lung, kidney, stomach, bone tissue (*femur and lumbar spine*) or liver, whereas primary tumor tissues themselves (s.c. tumor) gave strong signals (*columns*). Data are shown as RLU (relative light units), i.e. LU from luciferase assay normalized by protein concentration. The *black horizontal line* marks the detection limit for metastatic lesions in individual tissues

In vivo effect of GemLip treatment on primary orthotopic LNCaP PCa tumor xenografts

The orthotopic LNCaP PCa model was used for studying anti-metastatic and anti-tumoral effects of chemotherapeutic intervention by liposomal gemcitabine (GemLip). Animals were selected from originally 50–60 orthotopically implanted mice. The animals were randomized by luminescence imaging into the three treatment groups (ten mice per group), eliminating the largest or the smallest primary tumors. Treatment started 5 days after randomization according to the scheme described above (Methods), roughly on day 28 after orthotopic implantation, and was performed three times.

The in vivo drug side effects and drug-induced toxicity were followed up by monitoring the general health situation (scrubby coat) and body weight reduction (>20%) of the animals (Fig. 5a). As shown in Fig. 5a, SCID mice bearing orthotopic LNCaP PCa xenografts showed a general loss of weight during tumor growth by 11–20% ($P < 0.001$) compared to weight before tumor implantation—a cachexia-like outcome which occurred

Table 1 Organ distribution of metastatic lesions (mean RLU values) and number of untreated metastatic animals in the orthotopic LNCaP PCa model

	LN	Duo	SP	Lung	Kidney	Sto	Femur	LuSp	Liver
Mean RLU[a]	1,878,851	763,830	217,490	112,437	20,359	16,287	7,301	13,879	9,437
Range	1,758–4,732,603	3,326–2,510,953	1,504–679,480	2,877–273,003	1,951–83,309	2,406–37,952	1,541–23,558	1,545–43,831	1,872–35,740
No. of animals[b]	7/9	4/9	6/9	8/9	9/9	6/9	6/9	7/9	7/9

Lymph node (LN), duodenum (duo), spleen (Sp), lung, kidney, stomach (Sto), femur, lumbar spine (LuSp), and the liver are potential target organs for metastatic lesions

[a] Mean RLU of animals with metastasis

[b] All animals with RLU < 1,500 were counted as metastases-free by our assay (9 animals—in the vehicle control group one animal died out of other than experimental reasons)

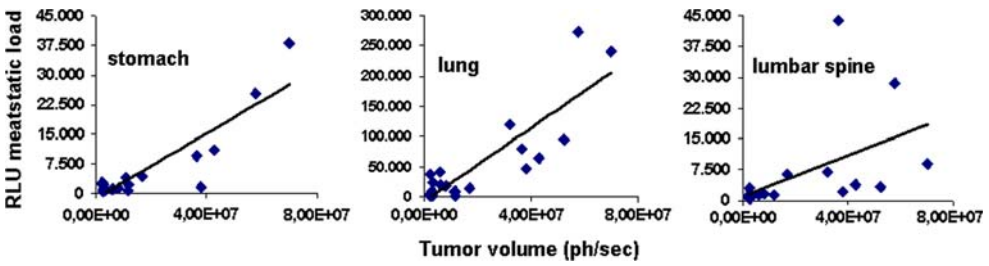

Fig. 4 Correlation of final tumor size and metastatic burden in individual tissues. The range of metastatic burden in individual tissues was generally very high (see also Table 1), and the distribution of metastatic lesions (Fig. 4: mean RLU) shows a significant correlation to the final primary tumor volume in individual animals defined by in vivo imaging (Fig. 4, ph/s) or by tumor volumes and weight, respectively (not shown). The correlation varied in individual tissues [stomach ($R = 0.887$; $P < 0.0001$), lung ($R = 0.870$; $P < 0.0001$), lumbar spine ($R = 0.510$; $P = 0.0181$)] but was significant in all investigated tissues (not shown)

independently of treatment also in the vehicle control group. Similar weight loss was also observed with subcutaneously growing LNCaP tumors (data not shown).

Tumor growth during GemLip treatment was monitored once weekly by luciferase in vivo bioluminescence as photons per second (Fig. 5b). Treatment of orthotopically growing LNCaP xenografts resulted in statistically significant reduced light signals (on day 19 and day 26 of treatment) in the GemLip group (8 mg/kg), reflecting a significant growth inhibition by 83.9 ± 6.4% ($P = 0.009$). Similar effects were seen with 360 mg/kg conventional Gemc, reducing tumor growth by 70.9 ± 13.5% ($P = 0.017$) relative to the vehicle.

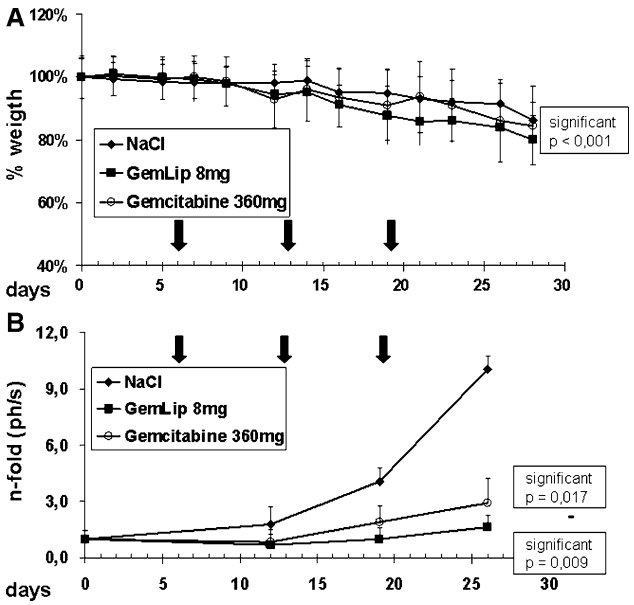

Fig. 5 Monitoring of drug effects and animal health during GemLip chemotherapy in orthotopic LNCaP xenografts. SCID mice bearing orthotopic LNCaP PCa xenografts were weighed 3 times weekly (**a**) and the results are plotted graphically for the treatment period as percentage of baseline weight before therapy (=100%) ±SD. All groups displayed a significant ($P < 0.001$) reduction of the body weight (baseline weight day 0: 26.25 ± 1.80 g) by 16.1 ± 10.8% on day 28 which was independent of whether the mice were treated once weekly (marked by the arrows) with the drugs GemLip (8 mg/kg) or gemcitabine (360 mg/kg), or if they received the vehicle control (physiological NaCl). This cachexia-like outcome was also observed in ectopic subcutaneous xenograft bearing animals (data not shown). Tumor growth (**b**) was monitored once weekly by luciferase bioluminescence in vivo imaging using the NightOwl LB981 CCD camera system (Berthold, Bad-Wildbach, Germany) as photons per second ± SD and plotted graphically as *n*-fold of bioluminescence before therapy. Treating orthotopically growing LNCaP xenografts resulted in significantly reduced light signals (on day 19 and day 26) in the GemLip ($P = 0.009$) and the gemcitabine ($P = 0.017$) group. Growth inhibition was 83.9 ± 6.4 and 70.9 ± 13.5%, respectively, of the vehicle. Necropsy was performed 2 days after final luminescence imaging

GemLip and metastatic lesions in primary orthotopic LNCaP PCa xenografts

In the next step we characterized anti-metastatic effects of the treatment. Scatter plots (Fig. 6) representing the signals of individual mice in the experimental groups and the means are shown in RLU normalized by protein values. Comparing untreated and treated animals in respective tissue groups (Fig. 6) medication with GemLip (8 mg/kg) significantly reduced the metastatic progression into the lymph nodes ($P = 0.047$), lung ($P = 0.015$), kidney ($P = 0.045$), and stomach ($P = 0.036$) whereas 360 mg/kg gemcitabine significantly reduced metastasis only in lung (0.018) and kidney ($P = 0.044$).

However, comparing the metastatic burden in the other tissues (duodenum, spleen, femur, lumbar spine or liver), it became obvious that either metastatic burden (mean RLU) or total number of metastatic animals (Table 1supp) or both were—compared to untreated animals—strikingly reduced by GemLip and less so by Gemc treatment (Fig. 6). But even these strong differences were not statistically significant, probably because of the strong variation in distribution of metastases (mean RLU) in untreated animals (see Table 1; Fig. 6).

Discussion

In the present study we have validated the anti-metastatic efficacy of liposomal gemcitabine (GemLip) therapy in a metastatic LNCaP PCa model. Orthotopic implantation of prostate cancer cells was one way to establish clinically relevant animal PCa models accompanied by bone or other metastatic invasion [13, 15, 19].

Various experimental PCa models—induced e.g. by orthotopic, intravenous, intra-femoral injection, or by bone contact implantation—have already been used for the investigation and development of new systemic adjuvant therapies against advanced PCa [11–18, 40, 41]. A stable genetic labelling of tumor cells with markers such as GFP or luciferase thus significantly enhanced in vivo or in vitro locating of metastases [18, 33, 42, 43]. Recently, two groups have reported even subcutaneously transplanted PCa cells to metastasize in a manner detectable by sensitive bioluminescence imaging or by quantitative real-time PCR [18, 33].

Using strongly luciferase/GFP fusion protein expressing LNCaP cells, a total of 1,000–10,000 cells per tissue piece could be detected. We have shown that orthotopic but not ectopic LNCaP PCa xenografts do strongly metastasize into bone tissue (femur, lumbar spine), lymph node, or lung, and thus represent a model reflecting the clinical situation. In contrast to the data of others [18, 33], but

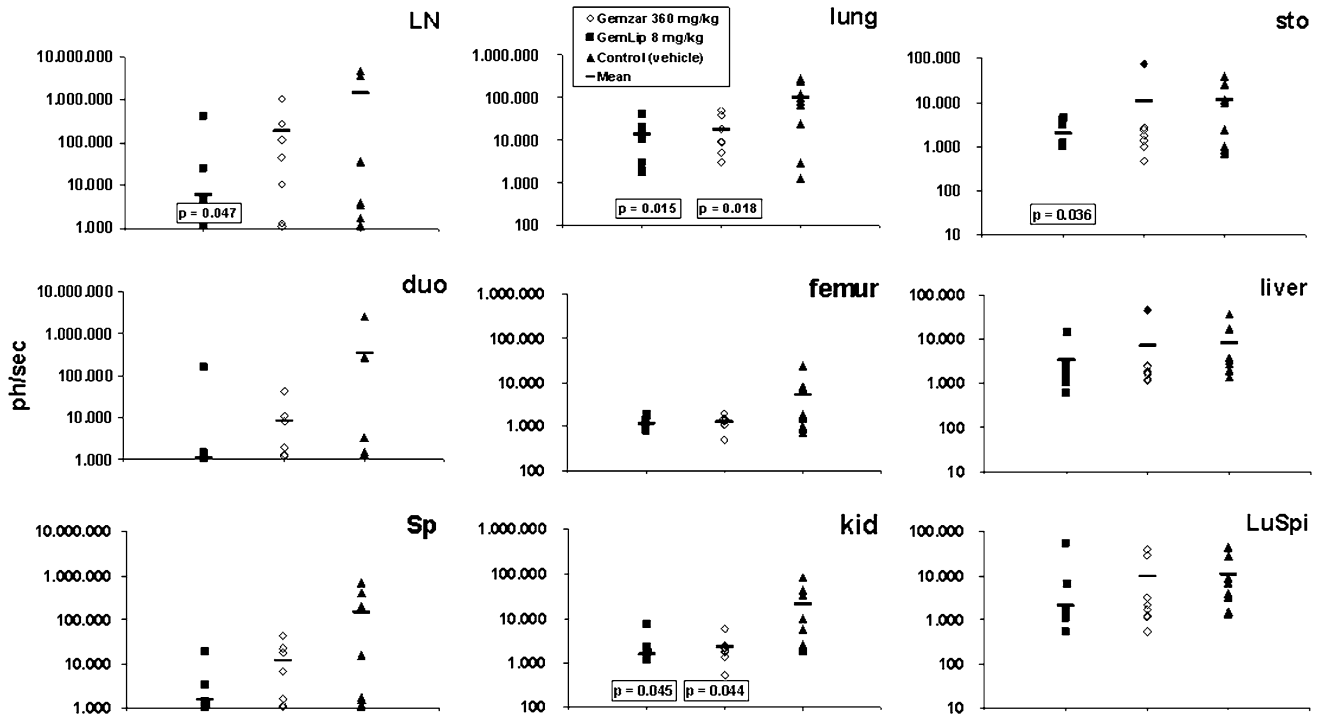

Fig. 6 Drug effects on metastatic lesions in orthotopic LNCaP PCa xenograft. In vitro luciferase assay results (endpoint analysis) from lymph node (LN), duodenum (duo), spleen (Sp), lung, femur, kidney (kid), stomach (sto), the liver and lumbar spine (LuSpi) as potential target organs show that LNCaP metastatic lesions can be detected in all investigated organs of individual SCID mice. Scatter graphs representing the signals of individual mice in the experimental groups and the means are shown in relative light units (RLU; $n = 10$) normalized by protein values. The metastatic burden in individual tissues was varying greatly with RLU values ranging from 1,000 to 10,000,000 (LN, duo, Sp), via 100–1,000,000 (lung, femur, kid) to 10–100,000 (sto, liver, LuSpi). GemLip treatment strongly reduced metastatic burden (mean RLU) in all tissues and the percentage of animals with metastatic lesion (Tab. 1supp). Because of the wide range of metastatic burden in untreated control animals this reduction was significant only in lymph nodes ($P = 0.047$), lung ($P = 0.015$), kidney ($P = 0.045$), and stomach ($P = 0.036$). Gemcitabine significantly reduced metastasis only in lung (0.018) and kidney ($P = 0.044$). Statistical analyses were performed using one-sided student's *t*-test with two samples of unequal variance

confirming results of Glinskii et al. [44], we could not find any metastatic lesion in ectopic, subcutaneously transplanted xenografts despite of the sensitive detection system. This difference might result either from different implantation materials, such as spongoid collagen scaffolds [18] versus Matrigel, or from different final growth periods of 14 weeks [33] versus 7 weeks in our study (Fig. 2). The take rate in the ectopic subcutaneous model was 95% using reconstituted extracellular matrix extract (Matrigel) as carrier, while carrier-free implantation (i.e. without Matrigel) only resulted in less than 10% of the animals (16 animals) developing subcutaneous tumors during the observation period (>12 weeks, data not shown). The carrier-free orthotopic implantation showed a significantly higher take rate of about 65%, indicating that there are strikingly different environmental conditions supporting tumor growth after orthotopic, but not ectopic, implantation.

This hypothesis is supported by the finding that administration of subcutaneously weak tumorigenic LNCaP cells resulted in increased tumor incidence (50–63%) when given simultaneously with different human prostate stromal cell lines [45]. In the orthotopic situation, the microenvironment of anterior prostate glands appears not only to facilitate tumor growth but also to induce metastatic dissemination (Fig. 2; 6). Since orthotopic tumor growth was accompanied by increased vascularisation and vascular leakage [20] (Fig. 2) this could be another factor advancing metastatic burden [43, 46]. Functional changes due to expression of cell adhesion molecules (CAM) can also modify cellular behaviour. Artificial MUC18 expression in transfected LNCaP cells has been shown to induce a four- to fivefold increase of in vitro motility and invasiveness, thus, could also foster tumor incidence as well as metastatic spread [47]. We have recently shown that co-culturing LNCaP cells with pieces of human prostate tissue resulted in enhanced expression of cell adhesion molecule CEACAM6 [48] (supplementary data Fig. 1supp), known to be associated with metastases, poor prognosis, and invasiveness in various tumors [49–51].

The metastatic burden in individual mice showed a significant correlation to the final tumor volumes (Fig. 4).

However, neither individual tumor volumes (Normality test failed: K–S Dist. = 0,283; $P < 0{,}001$), nor metastatic burden in individual tissues (failed: K–S Dist. = 0,411; $P < 0{,}001$) did pass the Normality Test (Kolmogorov–Smirnov), i.e. they do not display a Gaussian distribution. This reflects on one hand the high variation of the two parameters. On the other hand it demonstrates, although successfully implanting 1.00E+06 cells into the mouse prostates, the initial heterogeneity of tumor invasiveness and therefore metastatic dissemination. It results from the complex dependency on the heterogeneity of the PCa cells itself (e.g. a low and varying number of implanted tumor stem cells), as well as on varying factors in prostatic microenvironment and cellular-environmental interaction. These appear to influence tumor frequency or metastatic burden [52]. In the early phase of tumor implantation in our model this was characterized by two facts. First, the tumor implantation was successful only in about 65% of animals, i.e. in one-third of the animals none of the 1.00E+06 cells invaded and grew in prostate tissue. Second, a particularly strong reduction—in some cases a complete loss—of luciferase signalling was observed during the first 2 weeks between the first (at days 3–5 > 90% of animals were positive) and the second in vivo imaging in the immunodeficient animals, in some cases accompanied by a delayed re-appearance of tumor growth at later times (see: supplementary data Fig. 2supp).

Thus, this model seems to well reflect the clinical situation which is characterized by the fact that, at time of diagnosis, primary neoplasms are biologically heterogeneous and contain subpopulations of cells with different metastatic potentials [53–56]. The pathogenesis of a metastasis consists of many sequential steps that must be completed to produce clinically relevant lesions. During any of these steps, tumor cells interact with host factors in the microenvironment and will therefore will be subject to selection [57]. That there is actually a potential, selectable cellular heterogeneity also within PCa cell lines was shown by establishing LNCaP subclones displaying different tumor incidence or metastatic potential [58–61].

Using the present, clinically relevant orthotopic PCa model we could confirm former data on a soft tissue sarcoma and two orthotopic pancreatic cancer models [30–32] and demonstrate that a liposomal formulation of gemcitabine (GemLip) showed therapeutic efficacy also in PCa. GemLip at efficient doses of 8 mg/kg displayed not only significant anti-tumoral but also anti-metastatic effects. Non-liposomal Gemc is a chemotherapeutic drug which has shown only limited effects on human prostate cancer in vivo as yet [27–29, 62, 63] but which is efficient in various other cancer types (e.g. pancreas, non small cell lung cancer). Its entrapment into liposomes (GemLip) strikingly, about 45 times, enhanced efficacy of Gemc (efficient dose 360 mg/kg), probably resulting from protection from enzymatic degradation, prolonging its half-life to a great extent, as well as from enhanced accumulation of liposomal drugs within tumor tissues due to the enhanced permeability and retention effect (EPR), i.e. a passive targeting effect [30–32]. The EPR effect has been described in a broad variety of experimental tumor types [64–67], and mainly depends on tumor volume, vascularisation and leakage of tumor vessels. In fact, we could show strong vascularization [20] and highly enhanced vascular leakage in the orthotopic LNCaP model investigated in this study. EPR is also depending on the size and amount of the used liposomes, enhancement is higher the smaller and the more liposomes are present what is true for the liposomes we used ($\sim$40 nm in diameter, by an EE of 46%). In vivo allocation of GemLip was determined in various tissues performing fatty acid analysis by gas chromatography. Preliminary data showed a significant change in C18:0 and C18:1 fatty acid tissue content, indicating a liposome accumulation in vivo and concomitantly a better availability of the drug (P. Jantscheff and L. Taylor et al. unpublished data).

In contrast to former in vivo studies in a soft tissue sarcoma and two orthotopic pancreatic cancer models [30–32], conventional Gemc, too, had strong effects in the present orthotopic LNCaP PCa model, even if only at the 45-fold higher concentration of 360 mg/kg. Recently, we could show that tumor volume and vascularization are critical factors for the sensitivity of PC-3 PCa xenografts to conventional gemcitabine [68]. This might also be the case in the present study. Compared to subcutaneous (1.53 ± 0.65 cm^3) or pancreatic xenografts (1.69 or 1.94 cm^3 for MIA PaCa2 and AsPC1, respectively) [31, 32] the final tumor volumes in orthotopically implanted LNCaP mice were relatively small (0.70 ± 39 cm^3) and displayed an increased vascularization [20] (Fig. 2).

In summary, our data clearly show that metastatic spread of luciferase/GFP-expressing LNCaP xenografts after orthotopic implantation is a useful, clinically relevant animal PCa model for the investigation of new systemic adjuvant therapies and therefore might represent an important tool for investigating metastatic processes in various, e.g. bone, tissues, or for studying factors that regulate metastatic outgrowth. The observed heterogeneous metastatic spread seems to reflect the clinical situation quite well, characterized by the fact that at time of diagnosis, primary neoplasms often are biologically heterogeneous and contain subpopulations of cells with different metastatic potentials. And finally, in contrast to gemci ine, liposomal GemLip seems to be a chemotherapeutic drug potentially efficient in human PCa xenografts.

Acknowledgments This work was supported by the Dietmar Hopp Stiftung GmbH and the Kirstins Weg, Stiftung e.V.

References

1. Greenlee RT, Hill-Harmon MB, Murray T et al (2001) Cancer statistics, 2001. CA Cancer J Clin 51:15–36
2. Jemal A, Thomas A, Murray T et al (2002) Cancer statistics, 2002. CA Cancer J Clin 52:23–47
3. Bertz J, Giersiepen K, Haberland J et al (eds) (2006) Krebs in Deutschland. Häufigkeiten und Trends, 5th edn. Gesellschaft der epidemiologischen Krebsregister in Deutschland e.V. (GEKID) & Robert Koch-Institut (RKI), Saarbrücken
4. Vantyghem SA, Wilson SM, Postenka CO et al (2005) Dietary genistein reduces metastasis in a postsurgical orthotopic breast cancer model. Cancer Res 65:3396–3403
5. Weckermann D, Goppelt M, Dorn R et al (2006) Incidence of positive pelvic lymph nodes in patients with prostate cancer, a prostate-specific antigen (PSA) level of $\leq$ 10 ng/mL and biopsy Gleason score of $\leq$ 6, and their influence on PSA progression-free survival after radical prostatectomy. BJU Int 97:1173–1178
6. de Wit R (2008) Chemotherapy in hormone-refractory prostate cancer. BJU Int 101(Suppl 2):11–15
7. Nelson JB, Hedican SP, George DJ et al (1995) Identification of endothelin-1 in the pathophysiology of metastatic adenocarcinoma of the prostate. Nat Med 1:944–949
8. Wang Y, Xue H, Cutz JC et al (2005) An orthotopic metastatic prostate cancer model in SCID mice via grafting of a transplantable human prostate tumor line. Lab Invest 85:1392–1404
9. Lam JS, Yamashiro J, Shintaku IP et al (2005) Prostate stem cell antigen is overexpressed in prostate cancer metastases. Clin Cancer Res 11:2591–2596
10. Msaouel P, Pissimissis N, Halapas A et al (2008) Mechanisms of bone metastasis in prostate cancer: clinical implications. Best Pract Res Clin Endocrinol Metab 22:341–355
11. Sweeney P, Karashima T, Kim SJ et al (2002) Anti-vascular endothelial growth factor receptor 2 antibody reduces tumorigenicity and metastasis in orthotopic prostate cancer xenografts via induction of endothelial cell apoptosis and reduction of endothelial cell matrix metalloproteinase type 9 production. Clin Cancer Res 8:2714–2724
12. Wu TT, Sikes RA, Cui Q et al (1998) Establishing human prostate cancer cell xenografts in bone: induction of osteoblastic reaction by prostate-specific antigen-producing tumors in athymic and SCID/bg mice using LNCaP and lineage-derived metastatic sublines. Int J Cancer 77:887–894
13. Dumont P, Petein M, Lespagnard L et al (1993) Unusual behaviour of the LNCaP prostate tumour xenografted in nude mice. In Vivo 7:167–170
14. Yonou H, Kanomata N, Goya M et al (2003) Osteoprotegerin/osteoclastogenesis inhibitory factor decreases human prostate cancer burden in human adult bone implanted into nonobese diabetic/severe combined immunodeficient mice. Cancer Res 63:2096–2102
15. Rembrink K, Romijn JC, van der Kwast TH et al (1997) Orthotopic implantation of human prostate cancer cell lines: a clinically relevant animal model for metastatic prostate cancer. Prostate 31:168–174
16. Langley RR, Fidler IJ (2007) Tumor cell-organ microenvironment interactions in the pathogenesis of cancer metastasis. Endocr Rev 28:297–321
17. Talmadge JE, Singh RK, Fidler IJ et al (2007) Murine models to evaluate novel and conventional therapeutic strategies for cancer. Am J Pathol 170:793–804
18. Havens AM, Pedersen EA, Shiozawa Y et al (2008) An in vivo mouse model for human prostate cancer metastasis. Neoplasia 10:371–380
19. Stephenson RA, Dinney CP, Gohji K et al (1992) Metastatic model for human prostate cancer using orthotopic implantation in nude mice. JNCI 84:951–957
20. Graeser R, Chung DE, Esser N et al (2008) Synthesis and biological evaluation of an albumin-binding prodrug of doxorubicin that is cleaved by prostate-specific antigen (PSA) in a PSA-positive orthotopic prostate carcinoma model (LNCaP). Int J Cancer 122:1145–1154
21. Busby JE, Kim SJ, Yazici S et al (2006) Therapy of multidrug resistant human prostate tumors in the prostate of nude mice by simultaneous targeting of the epidermal growth factor receptor and vascular endothelial growth factor receptor on tumor-associated endothelial cells. Prostate 66:1788–1798
22. Cassinelli G, Lanzi C, Supino R et al (2002) Cellular bases of the antitumor activity of the novel taxane IDN 5109 (BAY59–8862) on hormone-refractory prostate cancer. Clin Cancer Res 8:2647–2654
23. Bergman AM, Pinedo HM, Talianidis I et al (2003) Increased sensitivity to gemcitabine of P-glycoprotein and multidrug resistance-associated protein-overexpressing human cancer cell lines. Br J Cancer 88:1963–1970
24. Cronauer MV, Klocker H, Talasz H et al (1996) Inhibitory effects of the nucleoside analogue gemcitabine on prostatic carcinoma cells. Prostate 28:172–181
25. Muenchen HJ, Quigley MM, Pilat MJ et al (2000) The study of gemcitabine in combination with other chemotherapeutic agents as an effective treatment for prostate cancer. Anticancer Res 20:735–740
26. Zhang C, Mattern J, Haferkamp A et al (2006) Corticosteroid-induced chemotherapy resistance in urological cancers. Cancer Biol Ther 5:59–64
27. Vogelzang NJ (2002) Future directions for gemcitabine in the treatment of genitourinary cancer. Semin Oncol 29:40–45
28. Pagliaro LC, Delpassand ES, Williams D et al (2003) A phase I/II study of strontium-89 combined with gemcitabine in the treatment of patients with androgen independent prostate carcinoma and bone metastases. Cancer 97:2988–2994
29. Rodney A, Dieringer P, Mathew P et al (2006) Phase II study of capecitabine combined with gemcitabine in the treatment of androgen-independent prostate cancer previously treated with taxanes. Cancer 106:2143–2147
30. Moog R, Burger AM, Brandl M et al (2002) Change in pharmacokinetic and pharmacodynamic behavior of gemcitabine in human tumor xenografts upon entrapment in vesicular phospholipid gels. Cancer Chemother Pharmacol 49:356–366
31. Bornmann C, Graeser R, Esser N et al (2008) A new liposomal formulation of gemcitabine is active in an orthotopic mouse model of pancreatic cancer accessible to bioluminescence imaging. Cancer Chemother Pharmacol 61:395–405
32. Graeser R, Bornmann C, Esser N et al (2009) Antimetastatic effects of liposomal gemcitabine and empty liposomes in an orthotopic mouse model of pancreatic cancer. Pancreas 38:330–337
33. Scatena CD, Hepner MA, Oei YA et al (2004) Imaging of bioluminescent LNCaP-luc-M6 tumors: a new animal model for the study of metastatic human prostate cancer. Prostate 59:292–303
34. Gossen M, Bujard H (1992) Tight control of gene expression in mammalian cells by tetracycline-responsive promoters. Proc Natl Acad Sci USA 89:5547–5551

35. Tardi C (1999) Vesikuläre Phospholipidgele: in vitro Charakterisierung, Autoklavierbarkeit, Anwendung als Depotarzneiform. PhD Thesis, Department of Pharmaceutical Technology, University of Freiburg, Germany
36. Brandl M, Massing U (2003) Vesicular phospholipid gels. In: Weissig V, Torchillin V (eds) Liposomes: a practical approach, vol 170. Oxford University Press, Oxford
37. Workman P, Balmain A, Hickman JA et al (1988) UKCCCR guidelines for the welfare of animals in experimental neoplasia. Lab Anim 22:195–201
38. Fastaia J, Dumont AE (1976) Pathogenesis of ascites in mice with peritoneal carcinomatosis. J Natl Cancer Inst 56:547–550
39. Roberts WG, Hasan T (1992) Role of neovasculature and vascular permeability on the tumor retention of photodynamic agents. Cancer Res 52:924–930
40. Kasman L, Lu P, Voelkel-Johnson C (2007) The histone deacetylase inhibitors depsipeptide and MS-275, enhance TRAIL gene therapy of LNCaP prostate cancer cells without adverse effects in normal prostate epithelial cells. Cancer Gene Ther 14:327–334
41. Zisman A, Ng CP, Pantuck AJ et al (2001) Actinomycin D and gemcitabine synergistically sensitize androgen-independent prostate cancer cells to Apo2L/TRAIL-mediated apoptosis. J Immunother 24:459–471
42. Maeda H, Segawa T, Kamoto T et al (2000) Rapid detection of candidate metastatic foci in the orthotopic inoculation model of androgen-sensitive prostate cancer cells introduced with green fluorescent protein. Prostate 45:335–340
43. Hoffman R (2002) Green fluorescent protein imaging of tumour growth, metastasis, and angiogenesis in mouse models. Lancet Oncol 3:546–556
44. Glinskii AB, Smith BA, Jiang P et al (2003) Viable circulating metastatic cells produced in orthotopic but not ectopic prostate cancer models. Cancer Res 63:4239–4243
45. Tuxhorn JA, McAlhany SJ, Dang TD et al (2002) Stromal cells promote angiogenesis and growth of human prostate tumors in a differential reactive stroma (DRS) xenograft model. Cancer Res 62:3298–3307
46. Downing S, Bumak C, Nixdorf S et al (2003) Elevated levels of prostate-specific antigen (PSA) in prostate cancer cells expressing mutant p53 is associated with tumor metastasis. Mol Carcinog 38:130–140
47. Wu GJ, Peng Q, Fu P et al (2004) Ectopical expression of human MUC18 increases metastasis of human prostate cancer cells. Gene 327:201–213
48. Jantscheff P, Reisen J, Sticker M et al (2005) GPI-linked CEACAM6 molecule expression in prostate cancer (abstract). Onkologie 28:50
49. Jantscheff P, Terracciano L, Lowy A et al (2003) Expression of CEACAM6 in resectable colorectal cancer: a factor of independent prognostic significance. J Clin Oncol 21:3638–3646
50. Duxbury MS, Ito H, Benoit E et al (2004) Overexpression of CEACAM6 promotes insulin-like growth factor I-induced pancreatic adenocarcinoma cellular invasiveness. Oncogene 23:5834
51. Blumenthal RD, Hansen HJ, Goldenberg DM (2005) Inhibition of adhesion, invasion, and metastasis by antibodies targeting CEACAM6 (NCA-90) and CEACAM5 (carcinoembryonic antigen). Cancer Res 65:8809–8817
52. Ariztia EV, Lee CJ, Gogoi R et al (2006) The tumor microenvironment: key to early detection. Crit Rev Clin Lab Sci 43:393–425
53. Mirchandani D, Zheng J, Miller GJ et al (1995) Heterogeneity in intratumor distribution of p53 mutations in human prostate cancer. Am J Pathol 147:92–101
54. Konishi N, Hiasa Y, Matsuda H et al (1995) Intratumor cellular heterogeneity and alterations in ras oncogene and p53 tumor suppressor gene in human prostate carcinoma. Am J Pathol 147:1112–1122
55. Navone NM, Olive M, Ozen M et al (1997) Establishment of two human prostate cancer cell lines derived from a single bone metastasis. Clin Cancer Res 3:2493–2500
56. Olapade-Olaopa EO, MacKay EH, Taub NA et al (1999) Malignant transformation of human prostatic epithelium is associated with the loss of androgen receptor immunoreactivity in the surrounding stroma. Clin Cancer Res 5:569–576
57. Fidler IJ, Kim SJ, Langley RR (2007) The role of the organ microenvironment in the biology and therapy of cancer metastasis. J Cell Biochem 101:927–936
58. Thalmann GN, Anezinis PE, Chang SM et al (1994) Androgen-independent cancer progression and bone metastasis in the LNCaP model of human prostate cancer. Cancer Res 54:2577–2581
59. McConkey DJ, Greene G, Pettaway CA (1996) Apoptosis resistance increases with metastatic potential in cells of the human LNCaP prostate carcinoma line. Cancer Res 56:5594–5599
60. Rhee HW, Zhau HE, Pathak S et al (2001) Permanent phenotypic and genotypic changes of prostate cancer cells cultured in a three-dimensional rotating-wall vessel. In Vitro Cell Dev Biol Anim 37:127–140
61. Freedland SJ, Pantuck AJ, Paik SH et al (2003) Heterogeneity of molecular targets on clonal cancer lines derived from a novel hormone-refractory prostate cancer tumor system. Prostate 55:299–307
62. Richards DA (2005) Chemotherapeutic gemcitabine doublets in pancreatic carcinoma. Semin Oncol 32:S9–S13
63. Boulikas T, Vougiouka M (2004) Recent clinical trials using cisplatin, carboplatin and their combination chemotherapy drugs (review). Oncol Rep 11:559–595
64. Gabizon AA, Shmeeda H, Zalipsky S (2006) Pros and cons of the liposome platform in cancer drug targeting. J Liposome Res 16:175–183
65. Yuan F, Dellian M, Fukumura D et al (1995) Vascular permeability in a human tumor xenograft: molecular size dependence and cutoff size. Cancer Res 55:3752–3756
66. Massing U (1997) Cancer therapy with liposomal formulations of anticancer drugs. Int J Clin Pharmacol Ther 35:87–90
67. Ludemann L, Grieger W, Wurm R et al (2005) Quantitative measurement of leakage volume and permeability in gliomas, meningiomas and brain metastases with dynamic contrast-enhanced MRI. Magn Reson Imaging 23:833–841
68. Jantscheff P, Esser N, Graeser R et al (2009) Liposomal gemcitabine (GemLip)-efficient drug against hormone-refractory Du145 and PC-3 prostate cancer xenografts. Prostate 69:1151–1163